Aberrant Mitosis in Fission Yeast Mutants Defective in Fatty Acid Synthetase and Acetyl CoA Carboxylase

Shigeaki Saitoh,* Kohta Takahashi,* Kentaro Nabeshima,* Yukiko Yamashita,* Yukinobu Nakaseko,* Aiko Hirata,‡ and Mitsuhiro Yanagida*

*Department of Biophysics, Faculty of Science, Kyoto University, Kitashirakawa-Oiwakecho, Sakyo-ku, Kyoto 606, Japan; and ‡Institute of Molecular and Cellular Biology, University of Tokyo, Bunkyo-ku, Tokyo 113, Japan

Abstract. Two fission yeast temperature-sensitive mutants, *cut6* and *lsd1*, show a defect in nuclear division. The daughter nuclei differ dramatically in size (the phenotype designated *lsd*, *l*arge and *s*mall *d*aughter). Fluorescence in situ hybridization (FISH) revealed that sister chromatids were separated in the *lsd* cells, but appeared highly compact in one of the two daughter nuclei. EM showed asymmetric nuclear elongation followed by unequal separation of nonchromosomal nuclear structures in these mutant nuclei. The small nuclei lacked electron-dense nuclear materials and contained highly compacted chromatin. The $cut6^+$ and $lsd1^+$ genes are essential for viability and encode, respectively, acetyl CoA carboxylase and fatty acid synthetase, the key enzymes for fatty acid synthesis. Gene disruption of $lsd1^+$ led to the lsd phenotype. Palmitate in medium fully suppressed the phenotypes of *lsd1*. Cerulenin, an inhibitor for fatty acid synthesis, produced the lsd phenotype in wild type. The drug caused cell inviability during mitosis but not during the G2-arrest induced by the *cdc25* mutation. A reduced level of fatty acid thus led to impaired separation of nonchromosomal nuclear components. We propose that fatty acid is directly or indirectly required for separating the mother nucleus into two equal daughters.

NUCLEAR division proceeds during the M-phase of the cell cycle and ensures that daughter nuclei will receive an equal set of chromosomes before the onset of cytokinesis. The mechanism and regulation of nuclear division are crucially important in the cell's transmission of genetic information to a descendant (Murray and Hunt, 1993; Koshland, 1994; Holm, 1994; Yanagida, 1995). Nuclear division has to be properly coordinated with cytokinesis (e.g., Fankhauser et al., 1993). If cytokinesis is triggered before the completion of nuclear division, the resulting cells may lose viability due to aberrant cytokinesis. In the fission yeast *Schizosaccharomyces pombe*, temperature-sensitive (ts)[1] mutants showing the occurrence of such uncoordinated cytokinesis have been isolated and called *cut* (*c*ell *u*ntimely *t*orn) mutants (Hirano et al., 1986; Samejima et al., 1993). In *cut* mutants, septation and subsequent cytokinesis take place although the preceding nuclear division is absent or abnormal. The cut^+ gene products are thus implicated in the proper coordination between nuclear division and cytokinesis.

In this study, the phenotypes of two fission yeast mutants, *cut6* (Hirano et al., 1986) and *lsd1* (isolated in the present study), and the gene products of $cut6^+$ and $lsd1^+$ were investigated. These mutants show infrequently the cut phenotype and very frequently a striking nuclear division phenotype resulting in daughter nuclei of unequal size (designated *lsd*, *l*arge and *s*mall *d*aughter). Thin-section EM of *lsd1* mutant cells confirmed that abnormal nuclear division occurred in the mutant cells. Gene cloning and nucleotide sequencing indicated that the gene products of $cut6^+$ and $lsd1^+$ were required for fatty acid synthesis. Fatty acid synthesis may be regulated so as to properly ensure nuclear and cell division. Cerulenin, a potent inhibitor of fatty acid synthetase (Inokoshi et al., 1994), produced the lsd phenotype in wild-type cells, similar to that seen in *lsd1* and *cut6*.

Results presented in this study show the requirement of fatty acid for normal nuclear division. If the level of intracellular fatty acid is not proper, the progression of nuclear and cell division is characteristically impaired, leading to the production of daughter nuclei whose sizes are dramatically different.

Address all correspondence to Mitsuhiro Yanagida, Department of Biophysics, Faculty of Science, Kyoto University, Kitashirakawa-Oiwakecho, Sakyo-ku, Kyoto 606, Japan. Tel.: (81) 75 753 4205. Fax: (81) 75 753 4208.

K. Takahashi's present address is Department of Molecular Biology, University of Geneva, Switzerland.

1. *Abbreviations used in this paper*: DAPI, 4′,6-diamidino-2-phenylindole; FISH, fluorescence in situ hybridization; SPB, spindle pole body; ts, temperature-sensitive; YPD, yeast extract/peptone/dextrose medium.

Materials and Methods

Strains and Media

The haploid *S. pombe* strains used were previously described (Hirano et al., 1986; Samejima et al., 1993; Takahashi et al., 1994). Rich yeast extract/peptone/dextrose medium (YPD) and minimal EMM2 media were used for the culture of *S. pombe* (Gutz et al., 1974). YPD medium containing 3.8–30 mg/ml palmitate and 1% Tween was used to examine the effect of palmitate. All plates contained 1.5% agar. Cell density of all cultures was estimated by a Sysmex Microcellcounter F800 (ToA Medical Electronics, Japan). Cell viability was determined by making appropriate dilutions of culture samples with distilled water, plating them, and counting the number of colonies after 3 d of incubation at 26°C. Viability was expressed as the ratio of viable colonies to the total number of cell bodies plated. A JE-6 elutriator rotor (Beckman Instruments, Inc., Palo Alto, CA) was used to collect early G2 cells, and synchronous culture was done at 33°C at a cell density of 6.5×10^5 per ml. A modified procedure of Costello et al (1983) was used for FACScan® analysis (Becton Dickinson & Co., Mountain View, CA).

Isolation of lsd1 Mutants

A collection of ts mutant strains (Takahashi et al., 1994) was searched for those showing the lsd phenotype at the restrictive temperature. Individual strains were first grown at 26°C, then shifted to 36°C, and observed after 4′,6-diamidino-2-phenylindole (DAPI) staining. Eleven strains exhibited a high frequency of the lsd phenotype. Another collection of ts strains (Hirano et al., 1986) was similarly screened, and three *lsd* mutant strains were obtained. Genetic analysis of these 14 ts strains showed that nine of them belong to the same genetic locus designated *lsd1*. The other strains were not investigated.

Gene Cloning by Transformation and Gene Disruption

An *S. pombe* genomic DNA library (Beach and Nurse, 1981) with the *Saccharomyces cerevisiae LEU2* marker was used. Transformation was done by the lithium method (Ito et al., 1983). Ts^+Leu^+ transformants were obtained, and plasmids were recovered from the Ts^+ Leu^+ cosegregants. Integration of cloned sequences onto the chromosome was performed by homologous recombination (Rothstein, 1983). For disruption of the $lsd1^+$ gene, pFAS2-100 containing the $lsd1^+$ gene was restricted, and 4.3-kb HpaI fragment was substituted by the *S. pombe* $ura4^+$ gene. The resulting plasmid pFAS2-210 was cleaved with SpeI, and the linearized fragment was used for transformation of a diploid 5A/1D (*h⁻/h⁺ leu1/leu1 ura4/ura4 his2/+ ade6-M210/ade6-M216*); stable Ura^+ heterozygous transformants were analyzed by tetrad analysis. Southern blotting was done on genomic DNAs of heterozygous diploids that had been digested with BglII using the SpeI fragment of $lsd1^+$ as the probe. For gene disruption of $cut6^+$, the BglII fragment in the coding region in plasmid pYY607 was substituted by the $ura4^+$ gene, and resulting plasmid pYY630 was linearized and used for transformation of a diploid strain. The resulting Ura^+ heterozygous diploids were sporulated and similarly analyzed by tetrad and genomic Southern hybridization.

Mapping the cut6 Locus

The integration vector pYC11 was used for homologous integration of the genomic DNA insert in pYY601 on the *S. pombe* chromosome (Takahashi et al., 1994). To locate map position of the $cut6^+$ gene, the ordered cosmid clones constructed for the *S. pombe* genome (Mizukami et al., 1993) were hybridized with the genomic DNA insert from pYY601. Hybridization occurred at the cosmid clones physically linked to the $cut5^+$ gene. The linkage between $cut5^+$ and $cut6^+$ was further verified by tetrad analysis of the cross between *cut6* and *cut5* (tetrad segregation, PD:NPD:TT=53:1:24). This result was consistent with the physical mapping data (Mizukami et al., 1993). The genomic DNAs carried by multicopy suppressor plasmids pYY602 and 609 were unlinked to the $cut5^+$ gene.

Nucleotide Sequence Determination

For nucleotide sequencing, Bluescript KS(+)SK(−) (Stratagene, La Jolla, CA) was used. Nucleotide sequences were determined by the dideoxy method (Sanger et al., 1977) using Taq DyeDeoxy™ Terminator Cycle Sequencing Kit and the 373A sequencer from Applied Biosystems (Foster City, CA).

Freeze-Substitution EM and Fluorescence Microscopy

The procedures for EM (Sun et al., 1992) and for DAPI (Adachi and Yanagida, 1989) were described previously. Cells were fixed with glutaraldehyde for DAPI stain. The method for fluorescence in situ hybridization (FISH) applicable to fission yeast cells was previously described (Funabiki et al., 1993). The digoxigenin-labeled rDNA probe (YIp10.4; Toda et al., 1984) was used.

Results

The lsd Phenotype Seen in cut6-621

Fission yeast *cut6-621* mutant cells (Hirano et al., 1986) showed aberrant nuclear division followed by septation and/or cytokinesis. Mutant cells cultured at the restrictive temperature (36°C) for 4 h and stained with DAPI displayed the cut phenotype in ~10% of cells (Fig. 1, *A* and *B*, *large arrows*). Another striking nuclear division phenotype (designated lsd) was found: DAPI-stained chromatin regions in the daughter nuclei differed in their size (Fig. 1, *A* and *B*, *arrowheads*). This asymmetric nuclear division was followed by either cytokinesis or septation (Fig. 1, small arrows). The lsd and cut phenotypes were infrequently seen at the permissive temperature (26°C) but not in wild type (not shown).

The frequency of the lsd phenotype seen in the binucleate cells of *cut6-621* was high, ~70% after 4 h at 36°C (the size of small nuclei determined by DAPI staining was 0.40–0.75 [average, 0.57] in comparison to that of large nuclei). Singly nucleate cells also contained nuclei varying in size (cells at bottom in Fig. 1 *A*), but they were not included in the quantitative analyses. The lsd phenotype in binucleate cells (~15% of the whole cell population) was more easily identified than it was in singly nucleate cells, as the two counterpart nuclei could be compared in the same cells. Anucleate cells (~1%) were produced as a result of septation in cells that had a displaced nucleus (a lower cell in the *upper panel* of Fig. 1 *B*), although their frequency was not high. The viability of *cut6-621* cells began to decrease after 3–4 h at 36°C and fell to 10% after 10 h (Fig. 1 *C*, *open circles*). The timing of this decrease roughly corresponded to the cell number increase (approximately twofold increase after 6 h at 36°C).

Isolation and Characterization of ts lsd1 Mutants

We isolated other fission yeast mutants that displayed the lsd phenotype by screening collections of ts mutants (see Materials and Methods). About 1,200 ts strains were individually cultured at 36°C for 2–6 h, and DAPI-stained cells were observed. 14 ts strains displaying the lsd phenotype at 36°C were isolated. They were crossed with each other, and nine of them were identified as belonging to the same genetic locus, designated *lsd1*. None of them was linked to *cut6*; other strains were not further investigated. All the *lsd1* strains thus isolated showed a similar phenotype at 36°C, so a representative strain, *lsd1-H518*, was used for further investigation.

The phenotype of *lsd1-H518* mutant cells cultured at 36°C for 6 h (Fig. 1 *D*) resembled that of *cut6-621*. Most cells displaying the lsd phenotype contained a septum. The relative intensity of DAPI staining in the small nuclei was

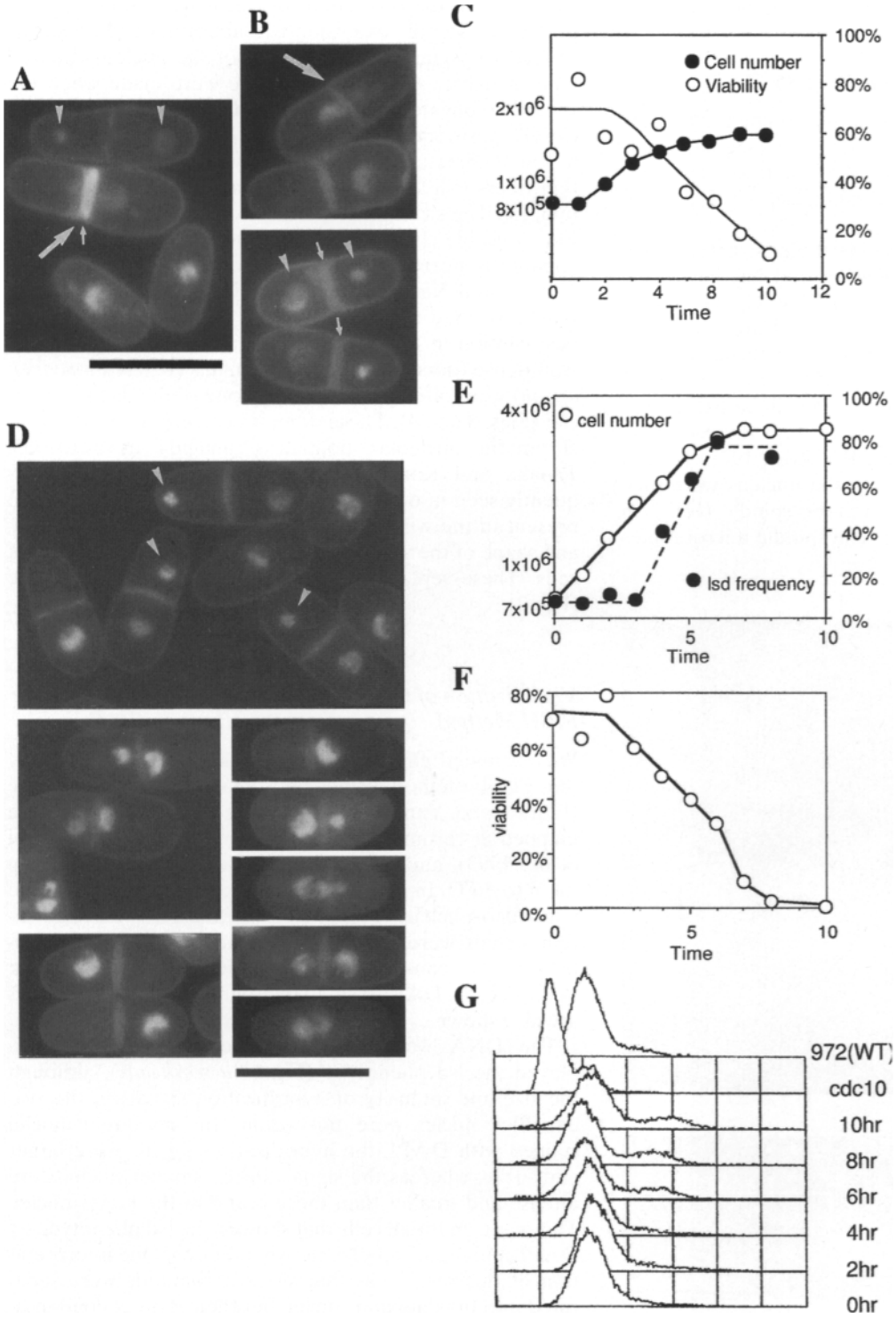

Figure 1. Phenotypes of *cut6-621* and *lsd1-H518* at the restrictive temperature. (*A* and *B*) *cut6-621* cells were cultured at 36°C for 4 h. Cells stained with DAPI showed the cut (*large arrows*) and the lsd phenotypes, (*arrowheads*). The thick septa are indicated by small arrows. The two cells at the bottom of *A*, which are products of a recent cytokinesis, contained nuclei of different sizes. Some cells contained the undivided nucleus displaced from the center of the cell and were septated (e.g., a lower cell in the upper panel of *B*). (*C*) Cell viability determined by plating decreased to 10% after 10 h at 36°C. The cell number increased approximately twofold after 8 h. (*D–G*) *lsd1-H518* mutant cells were cultured at 36°C for 0–10 h. DAPI-stained cells frequently showed the lsd phenotype after 6 h (*arrowheads* in *D*). In some cells the nucleus failed to divide but was displaced from the center of the cell, followed by the septum formation (*D*, *bottom left*). Various abnormalities in nuclear division are shown in the right bottom panel. Cells with thick septa were also frequent. The frequencies of binucleate cells displaying the lsd phenotype dramatically increased (*filled circles* in *E*). Cell number increased approximately fourfold, and then remained constant (*open circles* in *E*). Cell viability decreased after 2 h, and after 8 h, it was 0.5% of initial value (*F*). Cellular DNA content determined by the FACScan® method was 2C (*G*). A small fraction of cells contained 4C DNA after 6 h at 36°C. Bar, 10 μm.

high, as though chromosomes were highly condensed (Fig. 1 *D*, *arrowheads*, in *upper panel*). However, these cells were not in mitosis, judging from the presence of interphase cytoplasmic microtubules (Hagan and Hyams, 1988) seen by anti-tubulin staining (data not shown). Mutant cells infrequently (~2%) showed the cut phenotype (Fig. 1 *D*, *middle panel*). The nuclei bisected with septation were occasionally connected with a thin chromatin fiber running through the septum (Fig. 1; second and fourth cells in the *right bottom panel*; see also Fig. 3). Cell pairs containing a single displaced nucleus (Fig. 1 *D*, *bottom left*) were also seen.

Quantitative analysis indicated that the frequency of the lsd phenotype was high (80%) in the binucleate cells (Fig. 1 *E*, *filled circles*) after 6 h at 36°C, while the cell number had reached a plateau after an ~ fourfold increase. Cell viability was 40% at 5 h and <1% after 10 h (Fig. 1 *F*). The DNA contents determined by FACScan® were mostly 2C

at 36°C after 6 h (Fig. 1 *G*), although a small population of cells contained 4C DNA.

Thin-section EM of lsd1-H518 cells at 36°C

To obtain more information about the lsd phenotype, EM of the *lsd1-H518* mutant was performed (see Materials and Methods); mutant cells treated by the freeze-substitution method were thin sectioned and observed (Figs. 2, 3, and 4).

Several types of abnormalities in cellular structure associated with unequal nuclear division and uncoordinated septation/cytokinesis were observed at 36°C. (*a*) Mutant cells were partly or completely septated before nuclear division; the absence of nuclear division in those septated cells was verified by serial sections. Cells (1–4) in Fig. 2 would probably have progressed to the cut or lsd phenotype. In wild-type cells, the nucleus was fully divided at the onset of septation (McCully and Robinow, 1971; Tanaka and Kanbe, 1986). (*b*) Portions of the nucleus were protruded due to extension of the mitotic spindle (cell 3 in Fig. 2 *A*; also a cell in Fig. 2 *B*). The spindle microtubules were seen in the protruded regions (Fig. 2 *B*, *inset*). This protruding spindle extension was abnormal and appeared to lead to asymmetric separation of the nucleus. In wild type, daughter nuclei of equal size were made when the spindle elongated. (*c*) The divided nuclei were often closely positioned to the septum (Fig. 3). These nuclei were incomplete in division, as they were connected by the thin fibers (Fig. 3, *thin arrows*) that run through the septum. (*d*) The size and contents of divided daughter nuclei were variable (Figs. 3 and 4), but the daughter nuclei had apparently normal spindle pole bodies (SPBs) (Fig. 3 *B*; Tanaka and Kanbe, 1986). A series of sectioned micrographs verified the size difference in the daughter nuclei (see caption in Fig. 3). A striking fact was that the electron-dense (nonchromosomal) domains (Fig. 3, *short thick arrow*) were often present in only one of the daughter nuclei (Figs. 3 and 4). These domains correspond to the nonchromatin nucleolar domain (Yanagida et al., 1985; Tanaka and Kanbe, 1986). Small dense granules frequently seen in one of the nuclei (Figs. 3 and 4) were not present in the wild-type nuclei. (*e*) Positioning, direction, and shape of the septum were abnormal in a population of cells. These septa were thick particularly in the middle (Fig. 3).

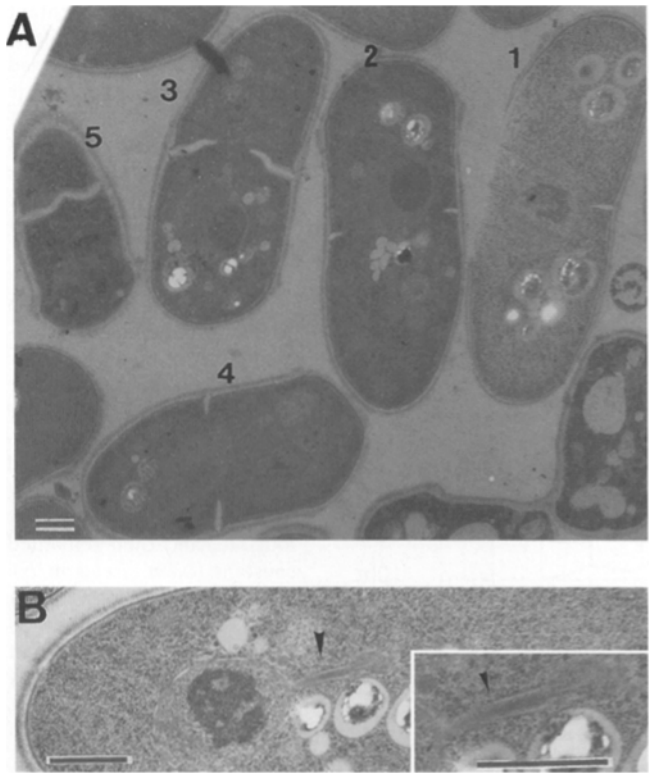

Figure 2. Thin-section electron micrographs of *lsd1-H518* mutant. Mutant cells were cultured at 36°C for 5 h, and specimens for the freeze-substitution method of EM were prepared (Sun et al., 1992). (*A*) Abnormal nuclei and septa seen in cells 1–4. These cells contained a single nucleus with a partly formed septum. Their septation was abnormal; in wild type, the septum was made only after the nucleus divided. The nucleus in cell 3 shows an abnormal protrusion with a partly formed septum, which was incorrectly directed and oblique to the cell axis. Aberrantly elongated nuclei were also seen as in 4. (*B*) The nucleus shows a short protruded structure (*arrowheads*) that contains the spindle microtubules. Bars: (*A* and *B*) 1 μm.

Visualization of Chromosome Segregation in lsd1 by the FISH Method

We examined chromosome segregation in *lsd1-H518* by the FISH method using ribosomal DNAs as a probe (Uzawa and Yanagida, 1992). The rDNA repeats were mapped at chromosome III (Toda et al., 1985; Mizukami et al., 1993), and cells were examined 5 h after shifting them to 36°C. In cells showing the cut phenotype and the undivided nucleus (Fig. 5, *arrows*), the rDNA hybridization signals were not separated and situated at the septated region, consistent with the failure of nuclear division in these cells. DAPI-stained micrographs of the same cells are also shown.

The rDNAs were separated in the mutant cells that displayed the lsd phenotype (Fig. 5, *arrowheads*), although the size and intensity of hybridization signals in the two daughter nuclei were not equal. In the larger nuclei stained with DAPI, the hybridization signals were larger and fuzzy, whereas the signals in the smaller nuclei were intense and smaller than those found in the larger nuclei. This was true for all cells that showed the lsd phenotype by DAPI staining (examples shown in Fig. 5). One interpretation of this result was that sister chromatids were separated into the daughter nuclei, but their state of condensation was strikingly different between the large and small daughter nuclei. The degree of condensation appeared to be severe in the small nuclei, whereas in the large nuclei, it was the same as that of wild-type nuclei (Fig. 5, *right bottom panel*; *wt*). Chromosome painting for the left arm of chromosome II by FISH (Saka et al., 1994) was used, and basically, the same results described above were obtained (data not shown). A unique cosmid probe used to examine separation of the centromeres in chromosome II by FISH verified the conclusion that sister chromatids were separated in cells showing the lsd phenotype.

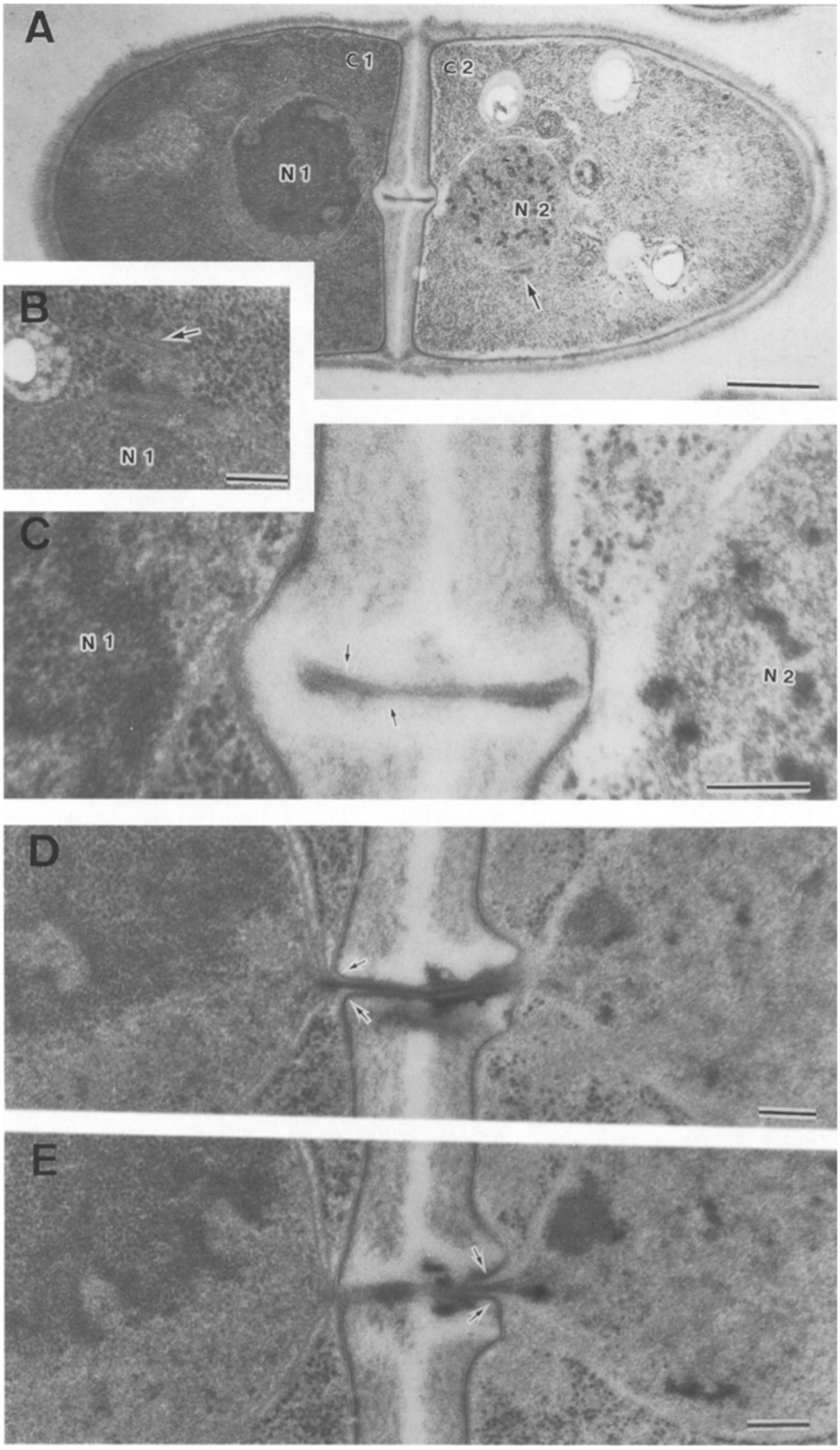

Figure 3. The cut phenotype seen in *lsd1* mutant. Abnormal nuclear division often accompanied septum formation. These serial sections represent a cell (*A–E*) showing the cut phenotype. The nuclei were not completely separated as the thin fiber-like structure (*thin arrows*) ran through the septum, which was apparently thicker than that of wild type (enlarged portions in *C–E*). The structure was connected to the nuclear envelopes in N1 and N2 (*D* and *E*). A series of sections clearly indicate that the N1 nucleus in the C1 cell is larger than N2 in C2: the N1 nucleus appeared in 30 sections, while the N2 nucleus was present in 20 sections. The larger nucleus N1 contained the electron-dense nucleolus. The SPBs were duplicated in this cell: one SPB (*arrow* in *B*) was present in the N1 nucleus, while the other SPB existed in the N2 nucleus of the same cell (*arrow* in *A*). Micrographs *A* and *B* were obtained from different thin sections. Bars: (*A*) 1 μm; (*B–E*) 0.2 μm.

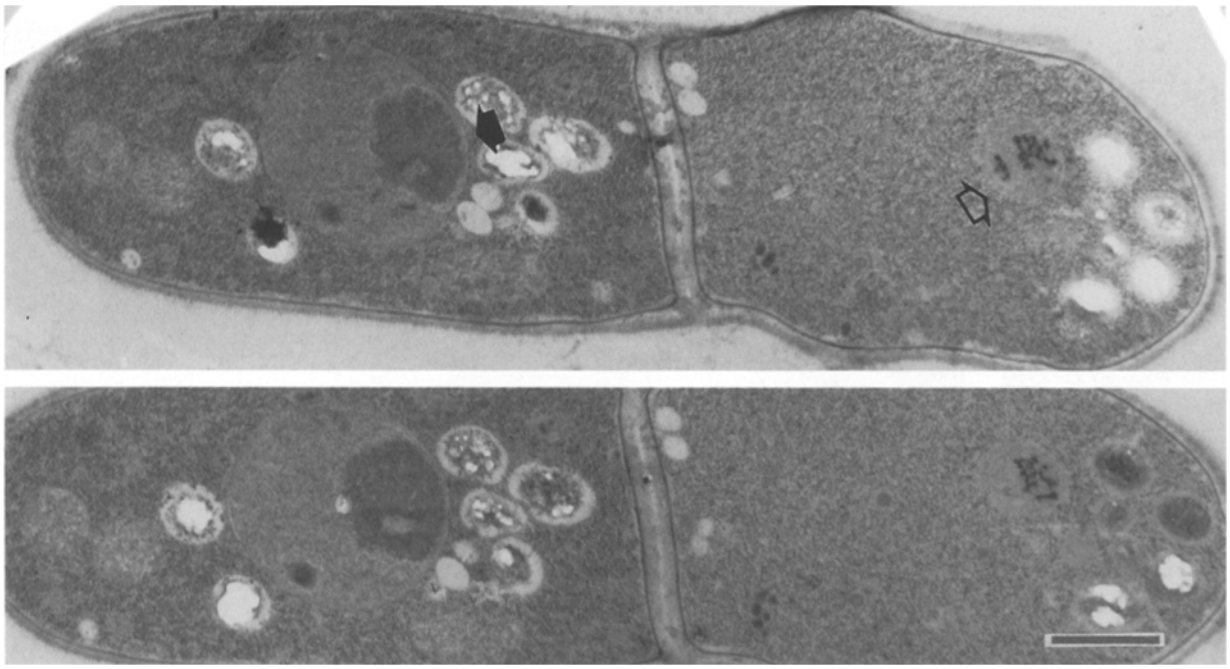

Figure 4. The lsd phenotype seen in two sections of the same cell. The electron-dense nonchromosomal region (*short thick arrow*) was localized in the larger daughter nucleus. The electron-dense dots (*open arrow*) were seen in the smaller daughter nucleus. Bar, 1 μm.

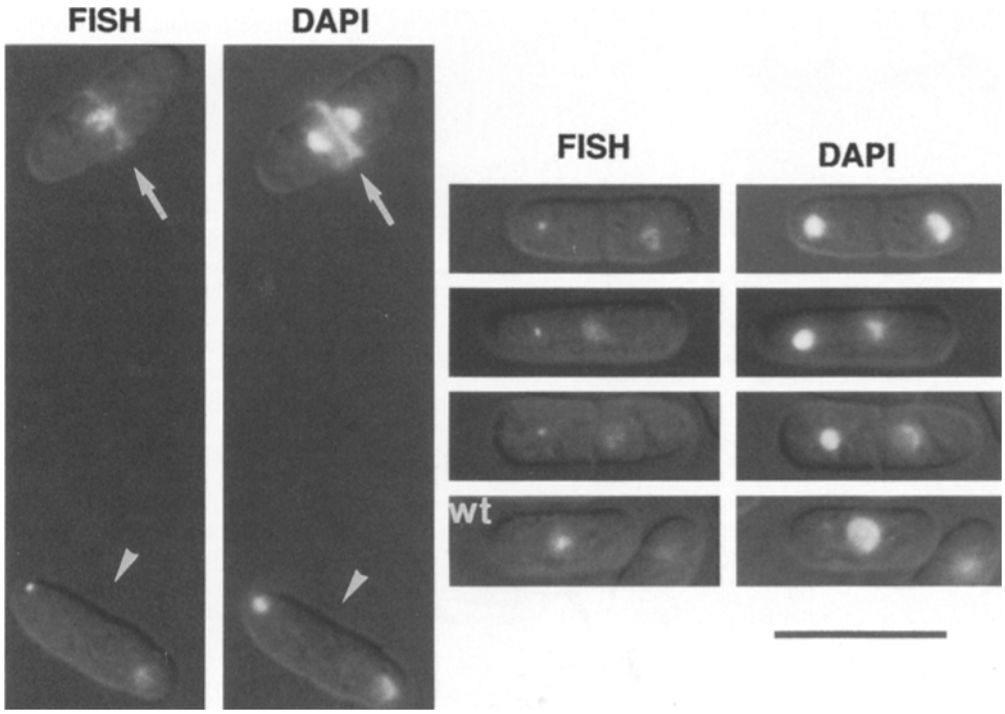

Figure 5. Visualization of chromosome separation in *lsd1-H518* mutant by the FISH method. *lsd1-H518* cells cultured at 36°C for 6 h were fixed and treated by the FISH method and DAPI staining. The probe used for hybridization was the rDNA repeating unit (Toda et al., 1984; Uzawa and Yanagida, 1992). DAPI-stained micrographs were taken in combination with Nomarski optics to display the shape of cells and the septum. In cells showing the cut phenotype, rDNAs were present at the septated cell (*arrows*, *left*). The rDNAs signal was compacted and intense in the small nuclei of cells that showed the lsd phenotype (*arrowheads*, *left*; cells, *right*). In all cells that revealed the lsd phenotype, the large nucleus gave an rDNA signal similar to wild-type cells, but the smaller nuclei gave a compact but intense signal. The wild-type control (*wt*) is shown in the right bottom panel. Bar, 10 μm.

The cut6⁺ Gene Encodes a Protein Similar to Acetyl CoA Carboxylase

To identify the gene product of *cut6⁺*, plasmid clones that complemented the *cut6-621* mutant were isolated from a genomic DNA library of *S. pombe* (see Materials and Methods). Three plasmids pYY601, 602, and 609, containing different genomic DNA inserts, were able to suppress the ts phenotype of *cut6-621*. pYY601 contained the *cut6⁺* gene, whereas the inserts in pYY602 and pYY609 were multicopy extragenic suppressors. This was shown by chromosomal integration of the plasmid sequences with the marker gene *LEU2* by homologous recombination. Tetrad analysis indicated that the integrated sequence of pYY601 was tightly linked to *cut6-621*, while those of pYY602 and pYY609 were not (data not shown). Further physical and genetic mapping described in Materials and Methods indicated that the *cut6⁺* gene was located near the *cut5⁺* gene on chromosome I.

A minimal functional clone complementing *cut6-621* was obtained by subcloning pYY601. The resulting plasmid (pYY622) contained a 6.4-kb NdeI–SalI fragment (Fig. 6 *A*). The nucleotide sequence was determined and deposited in the database (accession number D3413-3416). A large hypothetical polypeptide that was very similar to acetyl CoA carboxylase from *S. cerevisiae FAS3* (Al-Feel et al., 1992) covered the region essential for complementation. No other reading frame was found in the minimal functional clone. The Cut6 protein also shows homology to the *Ustilago maydis ACC* and rat ACACA genes, which also encode acetyl CoA carboxylase, are boxed in Fig. 6 *B*. Acetyl CoA carboxylase, which catalyzes the production of malonyl CoA from acetyl CoA, plays a key role in regulating fatty acid synthesis (Pelech et al., 1991; Chirala, 1992; Hardie and MacKintosh, 1992; Hasslacher et al., 1993; Woods et al., 1994; Ha et al., 1994).

The cut6⁺ Gene Was Essential for Viability

The *cut6⁺* gene in one of the two chromosomes of diploid was disrupted by one-step gene replacement (Fig. 6 *C*; see Materials and Methods). The 1.2-kb BglII fragment in the coding region was substituted with the *S. pombe ura4⁺* gene. The linearized plasmid was integrated onto the chromosome of a diploid by transformation, and resulting heterozygous Ura⁺ diploids were obtained. Genomic Southern hybridization verified gene disruption in the heterozygous diploids (data not shown). Tetrad analysis of sporulated

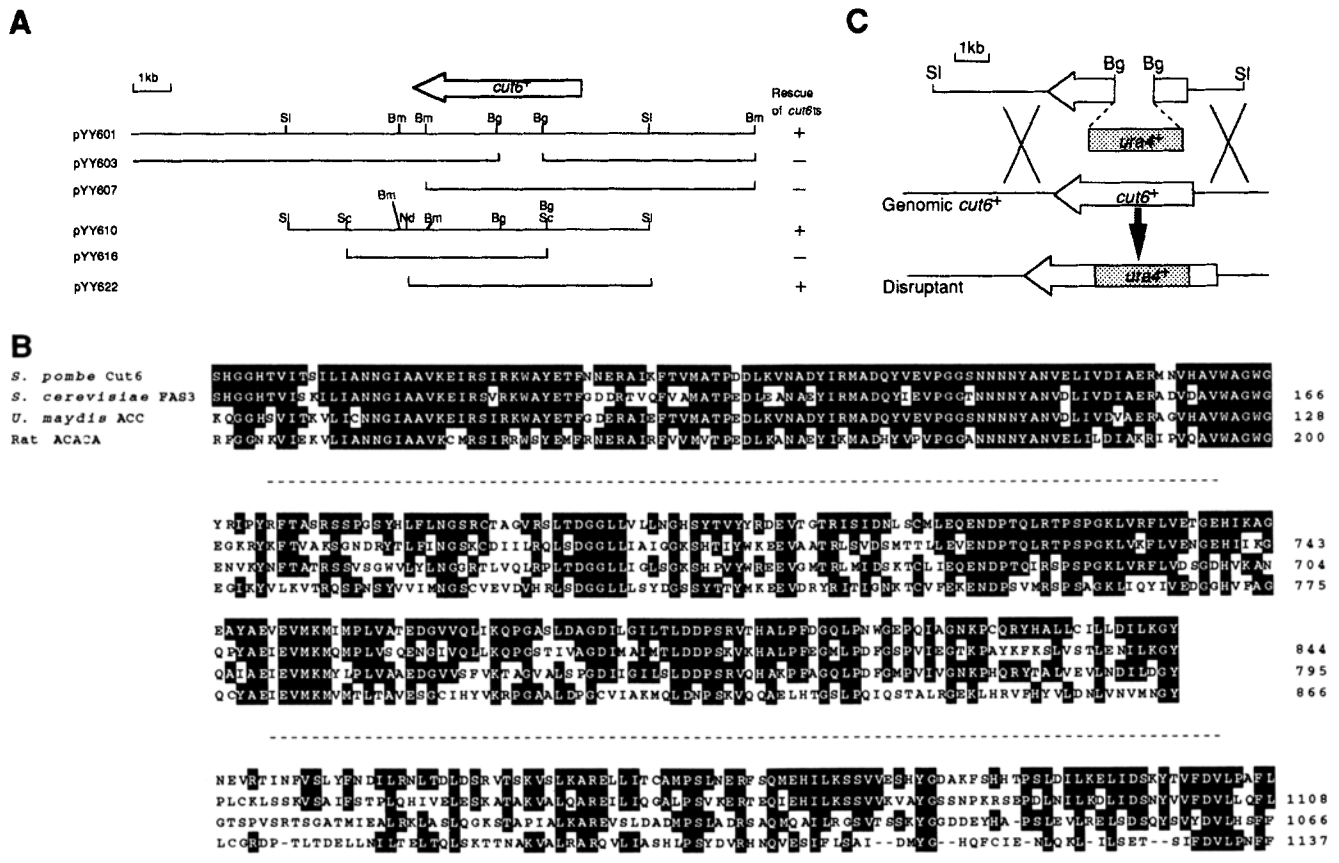

Figure 6. Cloning, sequencing, and gene disruption of the *cut6⁺* gene. (*A*) Plasmid pYY601 and a minimal subclone pYY622 complemented *cut6-621*. Nucleotide sequencing of pYY622 showed the presence of a large open reading frame highly similar to the *S. cerevisiae* acetyl CoA carboxylase. (These sequence data are available from EMBL/GenBank/DDBJ under accession number D83413-D83416.) (*Arrow*) Coding region of *cut6⁺*. (*B*) Amino acid sequence comparison of the predicted Cut6 sequence with the budding yeast Fas3 (Al-Feel et al., 1992), *U. maydis* (GenBank accession number Z46886), and rat (Lopez-Casillas et al., 1988) acetyl CoA carboxylase. (*C*) Strategy for the gene disruption of *cut6⁺*. The *S. pombe ura4⁺* gene was used to replace the BglII fragment in the coding region of the *cut6⁺* gene.

diploids showed two viable and two inviable spores. All the viable spores did not contain the marker gene and were Ura$^-$. The *cut6*$^+$ gene was thus essential for viability.

The lsd1$^+$ *Gene Encodes Fatty Acid Synthetase α-Subunit*

Two plasmids capable of complementing the ts phenotype of *lsd1-H518*, were obtained from the *S. pombe* genomic DNA library by transformation. Restriction mapping indicated that the inserts overlapped and derived from the same genomic region. Hybridization of the ordered cosmid bank (see Materials and Methods) showed that the complementing DNAs were closely linked to the *ppa1*$^+$ gene in the left arm of chromosome I (Mizukami et al., 1993). Consistent with this physical data, tetrad dissection data demonstrated a close linkage between *lsd1* and *ppa1* (PD: NPD:TT=27:0:0). The cloned DNAs should thus contain the *lsd1*$^+$ gene.

Subcloning was performed and a minimal complementing clone pFAS2-100 (7-kb-long SpeI fragment) was obtained (Fig. 7 *A*). Nucleotide sequencing of the entire SpeI fragment revealed a single long open reading frame. This hypothetical *lsd1*$^+$ gene encodes an 1,842-amino acid protein, strongly similar to the fatty acid synthetase subunit α (Fig. 7 *B*). The full nucleotide sequence was deposited to the DDBJ/EMBL (accession number D83412). Its predicted amino acid sequence (calculated mol wt., 202 kD) was ~60% identical to that of *S. cerevisiae FAS2* (Kuziora et al., 1983; Mohamed et al., 1988). Fatty acid synthetase catalyzes the synthesis of saturated long-chain fatty acids from acetyl CoA, malonyl CoA, and NADPH. The giant enzyme from budding yeast consists of two kinds of multifunctional polypeptide chains, α and β, and has the subunit composition of $\alpha_6\beta_6$ (producing a particle mass of 2,400 kD; Wieland et al., 1978, 1979).

Acetyl CoA carboxylase and fatty acid synthase are the key enzymes for the production of long-chain fatty acids.

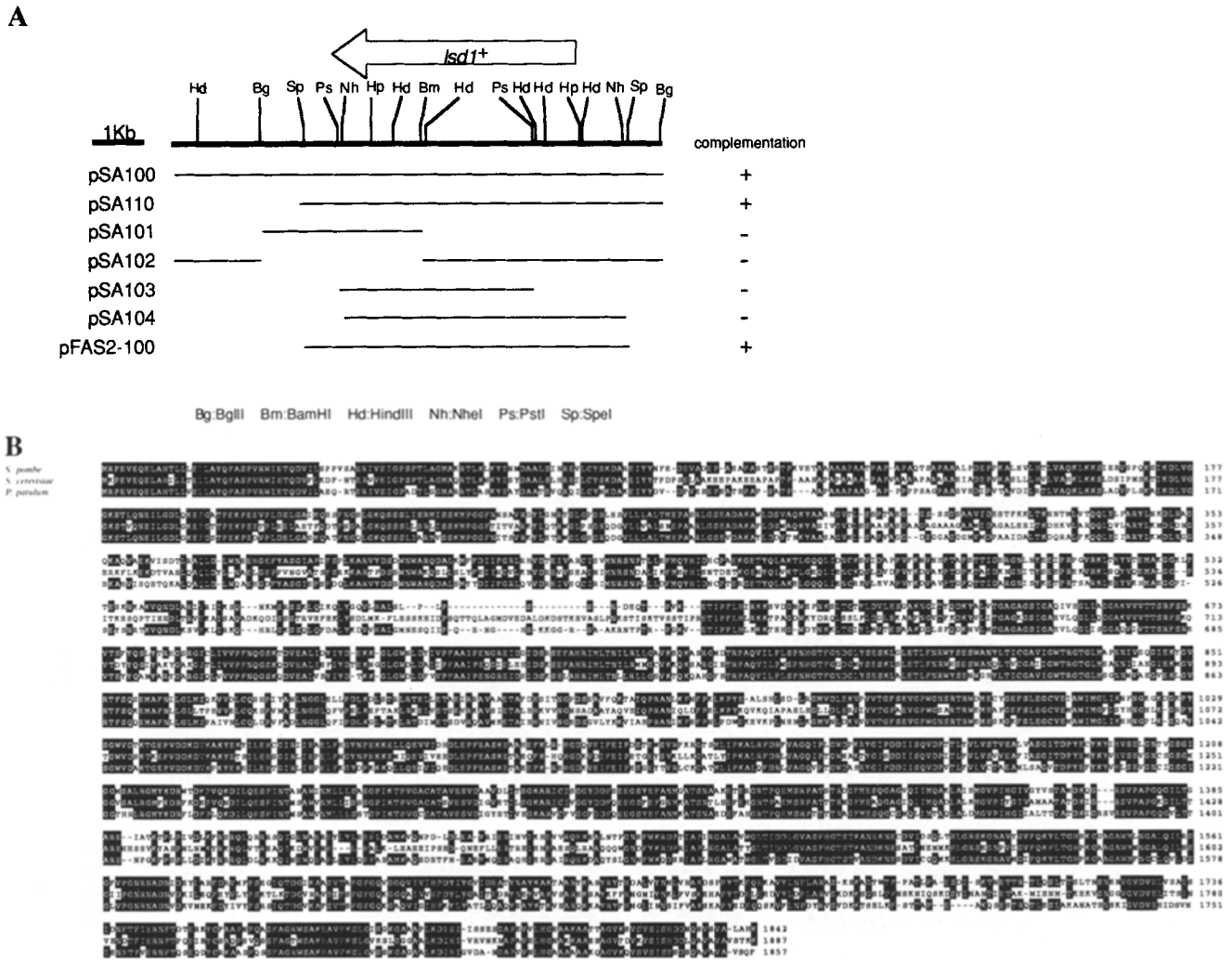

Figure 7. Cloning and sequencing of the *lsd1*$^+$ gene. (*A*) The *lsd1*$^+$ gene is adjacent to the *sds22*$^+$ gene (Ohkura and Yanagida, 1991). The minimal complementing fragment in pFAS2-100 contains the entire coding region. (*B*) The entire nucleotide sequence was determined. (These sequence data are available from EMBL/GenBank/DDBJ under accession number D83412.) The coding region of Lsd1 contained 1,842 amino acids (calculated mol wt, 202 kD) and was highly similar to the fatty acid synthetase subunit α. The coding region is 5,526 bp long. The comparison of the predicted amino acid sequence of *lsd1*$^+$ with *S. cerevisiae* Fas2 (1,894 amino acids; Mohamed et al., 1988) and *Penicillium patulum* Fas2 (1,857 amino acids; Wiesner et al., 1988) is shown.

The lsd and other phenotypes observed in *cut6* and *lsd1* will be discussed below in relation to the defect in fatty acid synthesis.

Gene Disruption of lsd1⁺ Produces the lsd Phenotype

The *lsd1⁺* gene was disrupted with one-step gene replacement (see Materials and Methods). The strategy of gene disruption is shown in Fig. 8 *A*. Heterozygous diploids containing one chromosome disrupted at the *lsd1⁺* gene were sporulated and resulting spores were dissected and germinated. Only the two Ura⁻ spores for each tetrad produced colonies, indicating that the *lsd1⁺* was essential for viability. The Ura⁺ spores were germinated but ceased to divide after several divisions (Fig. 8 *B*). 70% of the binucleate cells 48 h after germination showed the lsd phenotype with the septum formed at the center of the cell (Fig. 8 *C*). Micrographs of representative cells with the lsd phenotype are shown in Fig. 8 *D*. The lsd phenotype seen in ts *lsd1* mutant strains is therefore not allele specific.

Suppression of the ts lsd1 Phenotype by Palmitate

Knowing that the *lsd1⁺* gene encodes the fatty acid synthetase α subunit, we examined whether the ts phenotype of *lsd1* mutants was suppressed by the addition of fatty acid to the culture medium. As shown in Fig. 9, *lsd1-H518*, *-H265*, and *-H201* strains produced colonies at the restrictive temperature when they were plated on YPD containing 0.03% (30 mg/ml) palmitate and 1% Tween 20, a detergent for dissolving palmitate in the medium (Schweizer et al., 1986). Both palmitate and Tween 20 were necessary to rescue the ts phenotype; the size of the colonies was nearly normal. Mutant cells grown at 36°C in the presence of palmitate did not show the lsd phenotype. Wild-type colony formation was not affected by the addition of palmitate and Tween 20. The ts phenotype was thus produced because of the inability of mutant cells to supply a sufficient amount of fatty acid. *cut6-621* mutant cells were, however, not complemented by the addition of palmitate. (Fig. 9)

Cerulenin Produced the lsd and cut Phenotype in Wild Type

Cerulenin is an antibiotic produced by the fungus *Cephalosporium cacrulens* and is a known inhibitor of fatty acid synthesis (Funabashi et al., 1989); cerulenin blocks the reaction catalyzed by β-ketoacyl Acyl Carrier Protein (ACP) synthetase. We examined whether the drug inhibited the growth of *S. pombe*. Wild-type cells produced no colonies on YPD plates containing 10 μg/ml cerulenin. In liquid culture the number of wild-type cells increased approximately twofold at 33°C in the presence of cerulenin (Fig. 10 *A*, *top panel*). DAPI-stained wild-type cells in the

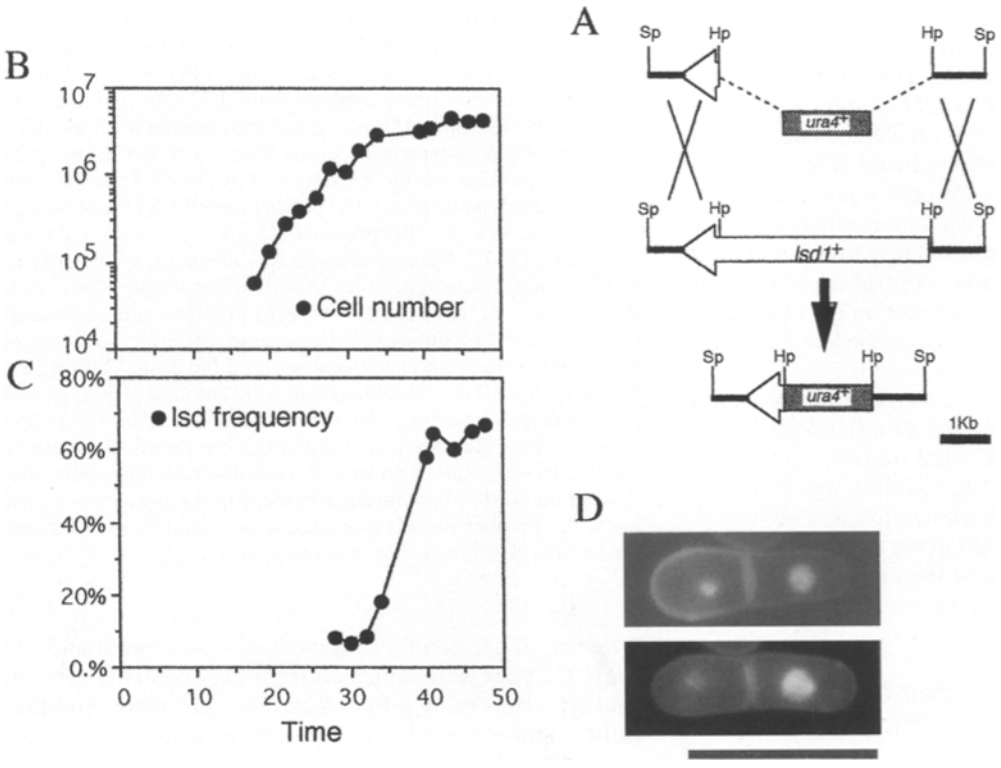

Figure 8. Gene disruption phenotype of the *lsd1⁺* gene. (*A*) Strategy for gene disruption of *lsd1⁺* is shown. The *S. pombe ura4⁺* gene was used to replace the 4.3-kb HpaI fragment in the *lsd1⁺* gene. The plasmid containing the disrupted gene was linearized and used for transformation of a diploid cell. The resulting heterozygous diploid transformant cells were examined by Southern hybridization to verify that they contained the disrupted gene. (*B–D*) Heterozygous diploid cells were sporulated, and the spores were germinated in the absence of uracil (only the spores carrying the disrupted gene were able to germinate). The cell number began to increase after 20 h and ceased around 34 h after approximately four to five cell divisions (*B*). The spores thus may contain fatty acid sufficient for this number of cell divisions. Cells showing the lsd phenotype increased after 20 h and reached the level of 70%. (*D*) DAPI-stained germinated cells displaying the lsd phenotype. Bar, 10 μm.

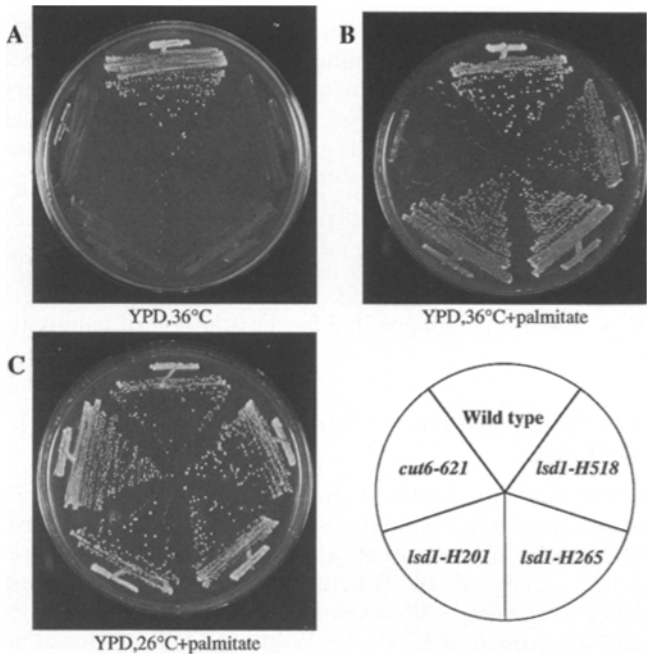

Figure 9. Rescue of *lsd1* mutants by palmitate. Five strains, wild type (HM123), *lsd1-H518*, *-H265*, *-H201*, and *cut6-621*, were plated on YPD in the presence or the absence of palmitate (30 mg/ml palmitate) at 36°C or 26°C. Only wild type produced colonies in the absence of palmitate at 36°C, whereas wild-type and *lsd1* strains produced colonies at 36°C in the presence of palmitate. The results indicated that the ts phenotype of three *lsd1* strains was rescued by the addition of palmitate to the culture medium.

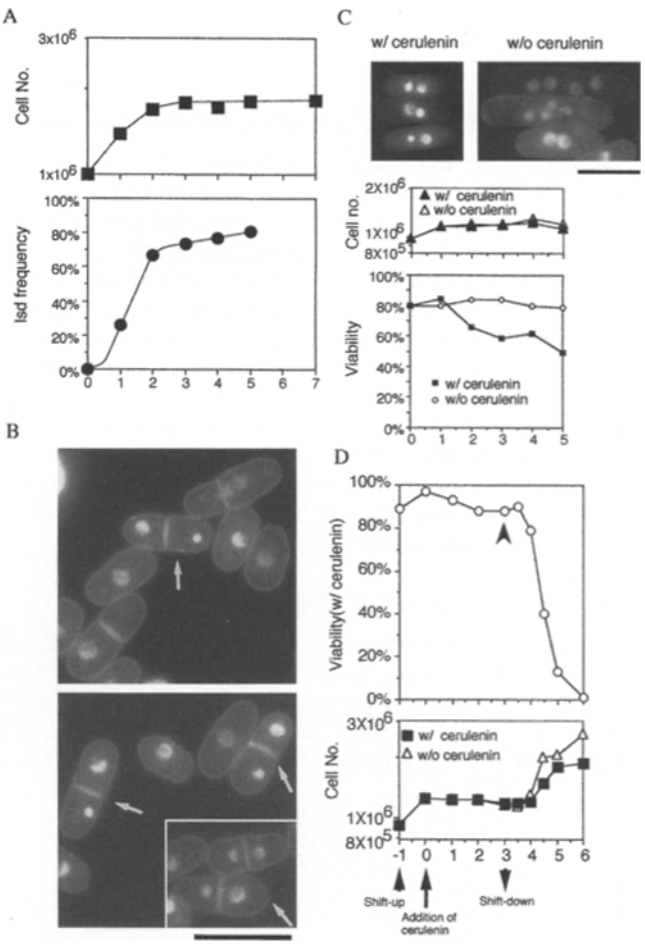

Figure 10. Effect of cerulenin on wild-type, *cdc11*, and *cdc25* mutant cells. (*A*) (*Upper panel*) The cell number increase of wild type 972 in the liquid YPD medium was measured at 33°C in the presence of 10 μg/ml cerulenin. Cells ceased to divide after the cell number increased 1.9-fold. (*Lower panel*) The frequency of the lsd phenotype measured in the same YPD liquid culture at 33°C for 5 h in the presence of cerulenin. Lsd cells first appeared 1 h after the addition of the drug and increased in level to ~80% after 5 h. (*B*) Wild-type cells cultured for 2 h at 33°C in the presence of 10 μg/ml cerulenin were stained by DAPI. Those showing the lsd phenotype (*arrows*). (*C*) (*Upper panel*) *cdc11* mutant cells cultured at 36°C in the presence of 10 μg/ml cerulenin and stained by DAPI. Nuclear division was blocked; ~70% cells remained singly nucleated, while 30% doubly nucleate after 5 h. In the absence of cerulenin, however, multiple nuclei formed. (*Lower panel*) Cell number in the presence of cerulenin increased at the same rate as *cdc11* in the absence of the drug. Viability was 50% after 5 h. (*D*) *cdc25* mutant cells were cultured at 36°C (−1 h), and cerulenin (10 μg/ml) was added at 0 h. The viability of *cdc25* cells remained high when arrested at G2, but rapidly decreased if *cdc25* cells were shifted down to the permissive temperature after 4 h and allowed to pass through mitosis. In the presence of cerulenin, the number of cells increased approximately twofold after the release (*filled rectangles*, *bottom panel*).

presence of cerulenin showed a high frequency (maximum 70% of binucleate cells) of the lsd phenotype at 33°C after 1–2 h (Fig. 10 *A*, *bottom panel*), similar to that produced in *cut6* and *lsd1* mutants (Fig. 10 *B*).

ts *cdc11* mutant cells are defective in septum formation at 36°C and produce multinucleate cells (Fig. 10 *C*, *top right panel*; Nurse et al., 1976). *cdc11* mutant cells were cultured at 36°C in the presence of cerulenin. The number of multinucleate cells was greatly reduced (Fig. 10 *C*, *top left*). The number of nuclei in many cells was either one or two (70% single nucleated and 30% binucleated) after 5 h, indicating that multiple rounds of nuclear division did not occur in the presence of cerulenin. Control *cdc11* mutants showed four (75%) or eight (25%) nuclei in the absence of cerulenin. However, cell viability decreased in the presence of cerulenin (Fig. 10 *D*, *bottom panel*).

Cell viability remained high in G2-arrested cells even if cerulenin was present (Fig. 10 *D*, *top panel*). *cdc25-22* mutant cells initially grown at 26°C were transferred to 36°C, and cerulenin was added after 1 h. Viability was kept high (Fig. 10 *D*, *top panel*), while cell elongation was not extensive. Then, the culture was shifted down to 26°C to release the arrest 3 h after the addition of the drug. Viability rapidly decreased as cells entered mitosis and cytokinesis (Fig. 10 *D*, *bottom panel*).

Lethal Effect of Cerulenin in Nuclear Division and Septation/Cytokinesis

Synchronous culture analysis of wild-type 972 cells in the presence of cerulenin (10 μg/ml) was performed at 33°C. Early G2 cells were collected from exponentially growing wild-type cells using a Beckman elutriator rotor, and then cultured for a period equivalent to two rounds of the cell cycle (Fig. 11). Cells were taken at 20-min intervals, and

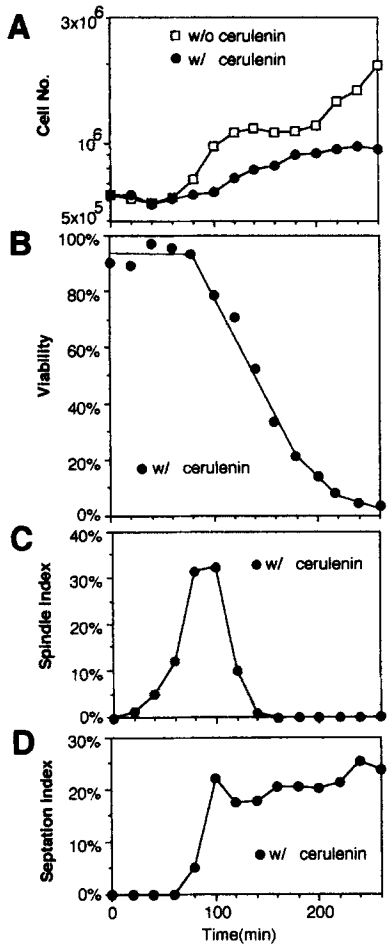

Figure 11. Synchronous culture of wild type in the presence of cerulenin. Wild type 972 cells were grown at 33°C, and early G2 cells were selected by elutriation centrifugation. Then they were synchronously cultured in the presence (10 μg/ml) or absence of cerulenin. (*A*) Cell number. (*Filled circles*) In the presence of cerulenin. (*Rectangles*) In the absence of cerulenin. (*B*) Viability was estimated by plating at 33°C. It decreased 100 min after the addition of cerulenin. (*C*) The spindle index was measured by counting the percentage of cells with spindles by fluorescence microscopy using anti-tubulin antibody TAT1. It peaked at 80–100 min, as did the wild-type control in the absence of the drug. (*D*) The septation index measured by Calcofluor staining increased after 100 min and maintained a high level. The wild-type control without the drug peaked at 100–120 min (not shown).

their cell number (Fig. 11 *A*, *open circles*; wild-type control, *rectangles*), viability by plating (Fig. 11 *B*), the spindle index by anti-tubulin staining (Fig. 11 *C*), and the septation index by Calcofluor staining (Fig. 11 *D*), were determined.

Spindle formation appeared to occur at normal timing, and cell viability decreased after spindle formation. The septation index was abnormal, as it rose with normal timing but did not decrease, demonstrating that cell separation was greatly delayed. Cell number increased ~1.8-fold after 260 min. Judging from the results of cell viability, 50% of the cells were viable after their spindle had broken down, but most lost viability during septation or after cytokinesis. From these results we concluded that lethal events in the presence of cerulenin occur during nuclear division and septation/cytokinesis.

Discussion

We show that the fission yeast *cut6*$^+$ and *lsd1*$^+$ genes code for acetyl CoA carboxylase and fatty acid synthetase α chain, respectively. Gene disruption experiments indicate that these enzymes are essential for viability. A surprising finding is that nuclear division is characteristically impaired in the mutants *cut6* and *lsd1*, resulting in the lsd phenotype. As both enzymes are essential for fatty acid synthesis and the mutant phenotypes are highly similar, we conclude that a proper intracellular level of fatty acid is needed for the progression of nuclear division. To our knowledge, this is the first report to demonstrate an essential role for acetyl CoA carboxylase and fatty acid synthetase α chain in the progression of nuclear division. In the budding yeast *S. cerevisiae*, mutants defective in these enzymes were identified (Dietlein and Schweitzer., 1975; Knobling and Schweizer, 1975; Roggenkamp et al., 1980; Mishina et al., 1980; Hasslacher et al., 1993; Inokoshi et al., 1994), but no cell cycle analysis has been reported. In fatty acid–supplemented media, *fas1* and *fas2* mutants exhibited the same growth properties as wild-type cells. Gene cloning indicated that the *FAS2* gene encodes the α subunit of fatty acid synthetase (Mohamed et al., 1988), while the *FAS3/ACC1* gene codes for acetyl CoA carboxylase (Al-Feel et al., 1992; Hasslacher et al., 1993).

The *cut6* and *lsd1* mutations are recessive. The mutant enzymes may be inactivated at 36°C, reducing the rate of de novo fatty acid synthesis and eventually decreasing the intracellular concentration of fatty acid. This notion was supported by the observation that the *lsd1* mutations were suppressed by the addition of palmitate to the culture medium. Treating wild-type cells with cerulenin, an inhibitor of fatty acid synthetase (Funabashi et al., 1989), produced a phenotype similar to that of *lsd1* mutants. The cell viability of G2-arrested *cdc25* cells remained high in the presence of cerulenin but rapidly declined upon the release into mitosis. At a mechanistic level, this result could be interpreted in several ways: the concentration of fatty acid has to increase as cells pass through nuclear division; alternatively, the fatty acid concentration normally remains constant, but the rate of fatty acid consumption increases during mitosis due to the production of nascent membranous components such as the nuclear envelope or transport vesicles; or fatty acid was produced and consumed at a constant rate during the cell cycle, but its deprivation in the G2-arrested cells did not lead to lethality. Distinguishing amongst these possibilities will require measurements of fatty acids and metabolites during the cell cycle.

It is not understood why *cut6* mutation was not rescued by the addition of palmitate. *cut6-621* might be a tighter mutation than *lsd1*. Alternatively, acetyl CoA carboxylase has possibly an essential function other than fatty acid synthesis. In *S. cerevisiae*, the addition of palmitate fails to rescue the *acc1* null mutation (Hasslacher et al., 1993).

The reaction directed by acetyl CoA carboxylase in mammalian cells is regulated by hormones or the level of important metabolites such as AMP. AMP-activated pro-

tein kinase (Hardie and MacKintosh, 1992; Woods et al., 1994), which converts the carboxylase into an inactive form, might be cell cycle regulated, as AMP is a sensitive indicator of the energy status of the cell.

The lsd phenotype is a novel defect in nuclear division. We initially speculated that the differently sized nuclei in *lsd1* and *cut6* mutant cells arose from error in chromosome segregation that produced aneuploid nuclei. However, the results of FISH experiments showed that sister chromatids were correctly separated in those *lsd1* cells exhibiting the lsd phenotype, indicating that kinetochore and spindle functions were normal in these cells. Unexpectedly, the difference in the sizes of daughter nuclei was partly due to the different degree of chromosome condensation in the daughter nuclei; chromosomes were more compacted in the small nuclei, judging from the signals of rDNAs in the FISH experiments. The cause for this distinct condensation in the daughter nuclei, however, was not determined. We suggest that the lack of nonchromosomal nuclear structures in the small daughter nuclei might be responsible for their greater condensation. The unequal distribution of the nuclear pores, for example, might also lead to an asymmetric defect in nuclear import, possibly resulting in aberrant chromosome condensation.

EM confirmed the nuclear division defect in *lsd1* mutant cells. An elongated spindle was seen in the rodlike protrusion of the nuclear envelope. This nuclear protrusion was aberrant and not observed in wild-type nuclear division (McCully and Robinow, 1971; Tanaka and Kanbe, 1986). These abnormal nuclear divisions in *cut6* and *lsd1* mutants may cause unequal distribution of nuclear constituents into the daughter nuclei. Nuclear components such as the electron-dense region (nucleolar matrices) largely remained in the large nucleus, while the small daughter nuclei often showed dense dots. The lack of certain nuclear components in the small nucleus might result in the inability to resume decondensed chromosomal architecture. The missing components could be any of the nuclear components, or nuclear organelles such as scaffolds, matrices, and/or the envelope, and it is of significant interest to identify them.

The phenotype of *dcd1* (defective in chromosome decondensation; Sazer and Nurse, 1994; Demeter et al., 1995) in telophase was somewhat similar to the lsd phenotype, although both daughter nuclei in *dcd1* mutant cells were hypercondensed. *dcd1* and *pim1* (Matsumoto and Beach, 1991) mutations occurred in the same gene, whose product is similar to mammalian RCC1 (Nishitani et al., 1991). The Pim1/Dcd1 protein localizes to nuclear chromatin and possibly the nuclear envelope, and it is probably required for nuclear transport and chromosome decondensaton after mitosis in *S. pombe*. As a number of phenotypes observed in *pim1/dcd1* mutants (Matsumoto and Beach, 1991, 1993; Sazer and Nurse, 1994: Demeter et al., 1995) were not found in *lsd1* and *cut6* mutants (present and unpublished results), it is unlikely that the gene product function of Pim1/Dcd1 is directly under the control of fatty acid level.

The shortage of fatty acids in mitosis might affect the chemical nature of the newly made nuclear envelope, possibly resulting in the failure in forming the dumbbell-shaped nucleus. Defect in mitochondrial inheritance and movement by a mutation in fatty acid metabolism are reported (Stewart and Yaffe, 1991). Another possible implication is that certain lipids might participate in forming nuclear skeletons other than the envelope. Alternatively, fatty acids might play an indirect role in acting in the generation of a second messenger. Various fatty acids are known to modify a number of small G proteins or subunits of heterotrimeric G proteins by isoprenylation or myristoylation (Fukada et al., 1990; Kokame et al., 1992; Casey, 1994), nuclear lamin (Georgatos et al., 1994), and protein tyrosine kinases (Koegl et al., 1994). To understand the phenotypes of *lsd1* and *cut6*, it is essential to determine the molecular consequences of the defect in fatty acid synthesis. In this regard, identification of the gene products for other *lsd* mutations is likely to be informative.

OA-519, a prognostic molecule found in tumor cells from breast cancer patients, was identified as fatty acid synthase (Kuhajda et al., 1994). Tumor fatty acid synthase is involved in the control of level and constituents of intracellular fatty acids, suggesting that abnormal regulation of fatty acid synthesis might cause the perturbation in cell division, leading to malignant tumors. One implication of the present study is that the shortage in fatty acid supply leads to a dramatic defect in the correct distribution of nuclear components during the cell cycle.

In fission yeast, the regulation of fatty acid synthesis in the cell cycle has been studied little. Two multicopy suppressors we obtained for *cut6-621* may shed light on the regulation of acetyl CoA carboxylase. One of these suppressors (designated Csx1; deposited in the DDBJ database, accession number D83417-D83418) encodes a protein similar to the budding yeast Ngr1 (negative growth regulator; Lee and Moss, 1993), Nam8 (Ekwall et al., 1992), and Pub1 (poly U-binding protein; Anderson et al., 1993). The amino acid identity in the region homologous to these RNA-binding proteins was 40–41%. Suppression by Csx1 suggests posttranscriptional regulation of acetyl CoA carboxylase. The other suppressor (designated Csx2; accession number D83419) revealed a hypothetical polypeptide that showed no similarity to known proteins.

In short, this work demonstrates the presence of a novel control ensuring equal redistribution process of nuclear components during the cell cycle, and the shortage in fatty acid supply during mitosis leads to a dramatic lethal defect in this process. The future work on how fatty acids and/or their metabolites are implicated in the nuclear division will lead to a better understanding in the mechanism of mitosis.

We thank Dr. Andrew Murray for his helpful comments and reading of this manuscript.

This work was supported by a grant (Specially Promoted Research) from the Ministry of Education, Science, and Culture of Japan.

Received for publication 22 March 1996 and in revised form 28 May 1996.

References

Adachi, Y., and M. Yanagida. 1989. Higher order chromosome structure is affected by cold-sensitive mutations in an *S. pombe* gene *crm1*$^+$ which encodes a 115-kD protein preferentially localized in the nucleus and at its periphery. *J. Cell Biol.* 108:1195–1207.

Al-Feel, W., S.S. Chirala, and S.J. Wakil. 1992. Cloning of the yeast FAS3 gene and primary structure of yeast acetyl-CoA carboxylase. *Proc. Natl. Acad. Sci. USA.* 89:4534–4538.

Anderson, J.T., M.R. Paddy, and M.S. Swanson. 1993. PUB1 is a major nuclear cytoplasmic polyadenylated RNA-binding protein in *Saccharomyces cerevi-*

siae. Mol. Cell. Biol. 13:6102–6113.
Beach, D., and P. Nurse. 1981. High-frequency transformation of the fission yeast *Schizosaccharomyces pombe. Nature (Lond.).* 290:140–142.
Casey, P.J. 1994. Lipid modifications of G proteins. *Curr. Opin. Cell Biol.* 6:219–225.
Chirala, S.S. 1992. Coordinated regulation and inositol-mediated and fatty acid-mediated repression of fatty acid synthase genes in *Saccharomyces cerevisiae. Proc. Natl. Acad. Sci. USA.* 89:10232–10236.
Costello, G., L. Rodgers, and D. Beach. 1986. Fission yeast enters the stationary phase G0 state from either mitotic G1 or G2. *Curr. Genet.* 11:119–125.
Demeter, J., M. Morphew, and S. Sazer. 1995. A mutation in the RCC1-related protein pim1 results in nuclear envelope fragmentation in fission yeast. *Proc. Natl. Acad. Sci. USA.* 92:1436–1440.
Dietlein, G., and E. Schweizer. 1975. Control of fatty-acid synthetase biosynthesis in *Saccharomyces cerevisiae. Eur. J. Biochem.* 58:177–184.
Ekwall, K., M. Kermorgant, G. Dujardin, O. Groudinsky, and P.P. Slonimski. 1992. The NAM8 gene in *Saccharomyces cerevisiae* encodes a protein with putative RNA binding motifs and acts as a suppressor of mitochondrial splicing deficiencies when overexpressed. *Mol. & Gen. Genet.* 233:136–144.
Fankhauser, C., J. Marks, A. Reymond, and V. Simanis. 1993. The *S. pombe cdc16* gene is required for maintenance of $p34^{cdc2}$ kinase activity and regulation of septum formation: a link between mitosis and cytokinesis? *EMBO (Eur. Mol. Biol. Organ.) J.* 12:2697–2704.
Fukada, Y., T. Takao, H. Ohguro, T. Yoshizawa, T. Akino, and Y. Shimonishi. 1990. Farnesylated gamma-subunit of photoreceptor G protein indispensable for GTP-binding. *Nature (Lond.).* 346:658–660.
Funabashi, H., A. Kawaguchi, H. Tomoda, S. Omura, S. Okuda, and S. Iwasaki. 1989. Binding site of cerulenin in fatty acid synthesis. *J. Biochem. (Tokyo).* 105:751–755.
Funabiki, H., I. Hagan, S. Uzawa, and M. Yanagida. 1993. Cell cycle–dependent specific positioning and clustering of centromeres and telomeres in fission yeast. *J. Cell Biol.* 121:961–976.
Georgatos, S.D., J. Meier, and G. Simos. 1994. Lamins and lamin-associated proteins. *Curr. Opin. Cell Biol.* 6:347–453.
Gutz, H., H. Heslot, U. Leupold, and N. Lopreno. 1974. *Schizosaccharomyces pombe. In* Handbook of Genetics 1. R.C. King, editor. Plenum Press, New York. 395–446.
Ha, J., S. Daniel, S.S. Broyles, and K.H. Kim. 1994. Critical phosphorylation sites for acetyl-CoA carboxylase activity. *J. Biol. Chem.* 269:22162–22168.
Hagan, I., and J.S. Hyams. 1988. The use of cell division cycle mutants to investigate the control of microtubule distribution in the fission yeast *Schizosaccharomyces pombe. J.Cell Sci.* 89:343–357.
Hardie, D.G., and R.W. MacKintosh. 1992. AMP-activated protein kinase- an archetypal protein kinase cascade? *Bioessays.* 14:699–704.
Hasslacher, M., A.V. Ivessa, F. Paltauf, and S.D. Kohlwein. 1993. Acetyl-CoA carboxylase from yeast is an essential enzyme and is regulated by factors that control phospholipid metabolism. *J. Biol. Chem.* 268:10946–10952.
Hirano, T., S. Funahashi, T. Uemura, and M. Yanagida. 1986. Isolation and characterization of *Schizosaccharomyces pombe cut* mutants that block nuclear division but not cytokinesis. *EMBO (Eur. Mol. Biol. Organ.) J.* 5:2973–2979.
Holm, C. 1994. Coming undone: how to undone a chromosome. *Cell.* 77:955–957.
Inokoshi, J., H. Tomoda, H. Hashimoto, A. Watanabe, H. Takeshima, and S. Omura. 1994. Cerulenin-resistant mutants of *Saccharomyces cerevisiae* with an altered fatty acid synthetase gene. *Mol. & Gen. Genet.* 244:90–96.
Ito, H., Y. Fukuda, K. Murata, and A. Kimura. 1983. Transformation of intact yeast cells treated with alkali cations. *J. Bacteriol.* 153:163–168.
Knobling, A., and E. Schweizer. 1975. Temperature-sensitive mutants of the yeast fatty-acid-synthetase complex. *Eur. J. Biochem.* 59:415–421.
Koegl, M., P. Zlatkine, S.C. Ley, S.A. Courtneidge, and A.I. Magee. 1994. Palmitoylation of multiple Src-family kinases at a homologous N-terminal motif. *Biochem. J.* 303:749–753.
Kokame, K., Y. Fukada, T. Yoshizawa, T. Takao, and Y. Shimonishi. 1992. Lipid modification at the N-terminus of photoreceptor G-protein alpha-subunit. *Nature (Lond.).* 359:749–752.
Koshland, D. 1994. Mitosis: back to the basics. *Cell.* 77:951–954.
Kuhajda, F.P., K. Jenner, F.D. Wood, R.A. Hennigar, L.B. Jacobs, J.D. Dick, and G.R. Pasternack. 1994. Fatty acid synthesis: a potential target for antineoplastic therapy. *Proc. Natl. Acad. Sci. USA.* 91:6379–6383.
Kuziora, M.A., J.H. Chalmers, M.G. Douglas, R.A. Hitzerman, J.S. Mattick, and S.J. Wakil. 1983. Molecular cloning of fatty acid synthetase genes from *Saccharomyces cerevisiae. J. Biol. Chem.* 258:11648–11653.
Lee, F.J., and J. Moss. 1993. An RNA-binding protein gene (RBP1) of *Saccharomyces cerevisiae* encodes a putative glucose-repressible protein containing two RNA recognition motifs. *J. Biol. Chem.* 268:15080–15087.
Lopez-Casillas, F., D. Bai, X. Luo, M.A. Hermodoson, and K. Kim. 1988. Structure of the coding sequence and primary amino acid sequence of acetyl-coenzyme A carboxylase. *Proc. Natl. Acad. Sci. USA.* 85:5784–5788.
Matsumoto, T., and D. Beach. 1991. Premature initiation of mitosis in yeast lacking RCC1 or an interacting GTPase. *Cell.* 66:347–360.
Matsumoto, T., and D. Beach. 1993. Interaction of the pim1/spi1 mitotic checkpoint with a protein phosphatase. *Mol. Biol. Cell.* 4:337–345.
McCully, E.K., and C.F. Robinow. 1971. Mitosis in the fission yeast *Schizosaccharomyces pombe*: a comparative study with light and electron microscopy. *J. Cell Sci.* 9:475–507.
Mishina, M., R. Roggenkamp, and E. Schweizer. 1980. Yeast mutants defective in acetyl-coenzyme A carboxylase and biotin: apocarboxylase ligase. *Eur. J. Biochem.* 111:79–87.
Mizukami, T., W.I. Chang, I. Gargavitsev, N. Kaplan, D. Lombardi, T. Matsumoto, O. Niwa, A. Kounousu, M. Yanagida, T.G. Marr, and D. Beach. 1993. A 13 kb resolution cosmid map of the 14 Mb fission yeast genome by nonrandom sequence-tagged site mapping. *Cell.* 73:121–132.
Mohamed, A.H., S.S. Chirala, N.H. Mody, W.Y. Huang, and S.J. Wakil. 1988. Primary structure of the multifunctional subunit protein of yeast fatty acid synthase derived from FAS2 gene sequence. *J. Biol. Chem.* 263:12315–12325.
Murray, A., and T. Hunt. 1993. The Cell Cycle: An Introduction. Oxford University Press, Oxford, UK. 251 pp.
Nishitani, H., M. Ohtsubo, K. Yamashita, H. Iida, J. Pines, H. Yasuda, Y. Shibata, T. Hunter, and T. Nishimoto. 1991. Loss of RCC1, a nuclear DNA-binding protein, uncouples the completion of DNA replication from the activation of cdc2 protein kinase and mitosis. *EMBO (Eur. Mol. Biol. Organ.) J.* 10:1555–1564.
Nurse, P., P. Thuriaux, and K. Nasmyth. 1976. Genetic control of the cell division cycle in the fission yeast *Schizosaccharomyces pombe. Mol. & Gen. Genet.* 146:167–178.
Ohkura, H., and M. Yanagida. 1991. *S. pombe* gene $sds22^{+}$ essential for a mid-mitotic transition encodes a leucine-rich repeat protein that positively modulates protein phosphatase-1. *Cell.* 64:149–157.
Pelech, S.L., J.S. Sanghera, H.B. Paddon, K.A. Quayle, and R.W. Brownsey. 1991. Identification of a major maturation-activated acetyl-CoA carboxylase kinase in sea star oocytes as p44mpk. *Biochem. J.* 274:759–767.
Roggenkamp, R., S. Numa, and E. Schweizer. 1980. Fatty-acid requiring mutant of *Saccharomyces cerevisiae* defective in acetyl-CoA carboxylase. *Proc. Natl. Acad. Sci. USA.* 77:1814–1817.
Rothstein, R.J. 1983. One-step gene disruption in yeast. *Methods Enzymol.* 101: 202–211.
Saka, Y., T. Sutani, Y. Yamashita, S. Saitoh, M. Takeuchi, Y. Nakaseko, and M. Yanagida. 1994. Fission yeast Cut3 and Cut14, members of a ubiquitous protein family, are required for chromosome consensation and segregation in mitosis. *EMBO (Eur. Mol. Biol. Organ) J.* 13:4938–4952.
Samejima, I., T. Matsumoto, Y. Nakaseko, D. Beach, and M. Yanagida. 1993. Identification of seven new cut genes involved in *Schizosaccharomyces pombe* mitosis. *J. Cell Sci.* 105:135–143.
Sanger, F., S. Nicklen, and A.R. Coulson. 1977. DNA sequencing with chain-terminating inhibitors. *Proc. Natl. Acad. Sci. USA.* 74:5463–5467.
Sazer, S., and P. Nurse. 1994. A fission yeast RCC1-related protein is required for the mitosis to interphase transition. *EMBO (Eur. Mol. Biol. Organ.) J.* 13:606–615.
Schweizer, M., L.M. Roberts, H.-J. Höltke, K. Takabayashi, E. Höllerer, B. Hoffman, G. Müller, H. Köttig, and E. Schweizer. 1986. The pentafunctional FAS1 gene of yeast: its nucleotide sequence and order of the catalytic domains. *Mol. & Gen. Genet.* 203:479–486.
Stewart, L.C., and M.P. Yaffe. 1991. A role for unsaturated fatty acids in mitochondrial movement and inheritance. *J. Cell Biol.* 115:1249–1257.
Sun, G.-H., A. Hirata, Y. Ohya, and Y. Anrakku. 1992. Mutations in yeast calmodulin cause defects in spindle polebody formation and nuclear integrity. *J. Cell Biol.* 119:1625–1639.
Takahashi, K., H. Yamada, and M. Yanagida. 1994. Fission yeast minichromosome loss mutants mis cause lethal aneuploidy and replication abnormality. *Mol. Biol. Cell.* 5:1145–1158.
Tanaka, K., and T. Kanbe. 1986. Mitosis in the fission yeast *Schizosaccharomyces pombe* as revealed by freeze-substitution electron microscopy. *J. Cell Sci.* 80:253–268.
Toda, T., Y. Nakaseko, O. Niwa, and M. Yanagida. 1984. Mapping of rRNA genes by integration of hybrid plasmids in *Schizosaccharomyces pombe. Curr. Genet.* 8:93–97.
Uzawa, S., and M. Yanagida. 1992. Visualization of centromeric and nucleolar DNA in fission yeast by fluorescence in situ hybridization. *J. Cell Sci.* 101: 267–275.
Wieland, F., E.A. Siess, L. Renner, C. Verfurth, and F. Lynen. 1978. Distribution of yeast fatty acid synthetase subunits: three dimensional model of the enzyme. *Proc. Natl. Acad. Sci. USA.* 75:5792–5796.
Wieland, F., C. Renner, C. Verfurth, and F. Lynen. 1979. Studies on the multienzyme complex of yeast fatty-acid synthetase. Reversible dissociation and isolation of two polypeptide chains. *Eur. J. Biochem.* 94:189–197.
Wiesner, P., J.J. Beck, K.-F. Beck, S. Ripka, G. Mueller, S. Luecke, and E. Schweizer. 1988. Isolation and sequence analysis of the fatty acid synthetase FAS2 gene from *Penicillium patulum. Eur. J. Biochem.* 177:69–79.
Woods, A., M.R. Munday, J. Scott, X. Yang, M. Carlson, and D. Carling. 1994. Yeast SNF1 is functionally related to mammalian AMP-activated protein kinase and regulates acetyl-CoA carboxylase in vivo. *J. Biol. Chem.* 269: 19509–19515.
Yanagida, M. 1995. Frontier questions about sister chromatin separation in anaphase. *Bioessays.* 17:519–526.